Rev. Adv. Mater. Sci. 33 (2013) 232-237

STUDY ON MICROSTRUCTURE AND IMPACT DUCTILITY OF SIMULATED WELD HAZ OF HIGH-STRENGTH WEAR-RESISTANT STEEL NM360

Zeng Gao and Jitai Niu

School of Materials Science & Engineering, Henan Polytechnic University, Jiaozuo, Henan, 454000, China

Received: October 17, 2011

Abstract. Due to the high carbon equivalent, high-strength wear-resistant steel NM360 which is widely used on excavating machinery always tends to welding crack during the manufacturing process. Heat affected zone (HAZ) is the weakest part in the welding joint. Most problems existing in HAZ such as harden quenching, cold crack, local brittleness as well as reheat crack are all related to the structure transformation and its products in HAZ material. In the present work, the impact ductility of NM360's HAZ under different cooling rate has been studied by using physical simulation method. And the impact ductility evolution mechanism has also been investigated according to the continuous cooling transformation (CCT) diagram which is taken from simulation. Microstructure, hardness, tendency of hardenability and possibility of generating cold crack of NM360's HAZ also can be predicted by CCT diagram. This study can provide useful data and lay experimental foundation for the research of weldability as well as the HAZ performance for NM360 steel.

1. INTRODUCTION

High-strength wear-resistant steel NM360, whose metallurgy mechanism is to increase the content of carbon and the other alloying elements, has been widely used in the field of excavating machinery. The combination property (including wear resistance, weldability and mouldability) has been greatly improved by the precipitation and phase transition during the thermal refining after rolling [1]. In welding manufacture, most problems existed in HAZ (such as harden quenching, cold crack, local brittleness as well as reheat crack) are all related to the structure transformation and its products in HAZ material. It's quite a difficult work to measure the phase transition in HAZ during experiment because the phase transition in welding joint is very fast, the temperature is high and the transition time is short. Physical simulation is an effective way to solve this kind of problem. It can amplify any positions in HAZ or some other places according to the thermal cycling curve. Subsequently the microstructure can be observed and the property can be tested conveniently. Amounts of repetitive experiments which were usually used before can be replaced by using the least physical simulation experiment. This can not only save a great quantity of manpower and material resources, but also provide a simple solution for complex problems which can not be investigated directly [2].

2. EXPERIMENTAL

2.1. Material

The experimental material is high-strength wear-resistant steel NM360. In order to improve its hardenability, temper resistance of martensite and refined grain, alloying elements Mn, Cr, Ni, Mo, B, Si, Al, and Ti have been added into NM360. Its

Corresponding author: Zeng Gao, e-mail: mrgaozeng@163.com

Table 1. Chemical compositions of NM360 steel (wt.%).

C	Si	Mn	P	S	Cu	Al
0.139	0.34	1.3	0.026	0.0078	0.039	0.031
Cr	Ni	Mo	Ti	B	N	
0.51	0.26	0.25	0.018	0.0016	0.0053	

Table 2. Mechanical properties of NM360 steel.

σ_bMPa	σ_SMPa	δ_5%	HB	A_{KV}J (Room Temperature)
≥1200	≥1000	10	360	42

chemical compositions and mechanical properties are shown respectively in Table 1 and Table 2. It can be seen from Table 2 that the hardness and strength of NM360 steel are excellent; however, its ductility property is not good enough. NM360 steel has been processed by thermal refining treatment after rolling and its microstructure is tempered sorbite with martensite characteristics. Microstructure of NM360 steel is shown in Fig. 1.

2.2. Experimental method

Thermal simulation test will be done on Gleeble-1500D. Specimen size is 11 mm × 11 mm × 90 mm which is decided by the heating system of the machine. In order to make the programming curve coincident with the actual thermal cycling curve, the span between grips varies with $t_{8/5}$. Fig. 2 illustrates the schematics of the test sample [2].

Table 3 shows the main parameters used in simulation experiment. They are introduced by the following items.

(1) Peak temperature T_p

T_p was selected for 1320 °C in consideration of the following factors.

1. Temperature for the coarse grain formation in HAZ ranges from 1200 to 1400 °C.
2. Temperature of fusion line distributes between 1300 and 1350 °C for low carbon steel and low alloy steel.
3. Gleeble-1500D will make 10~20 °C overshoot.

(2) Heating rate W_H

Heating rate W_H has a great influence on the phase transition temperature of A_{C1} and A_{C3} as well as the phase transition product and its feature. Measuring transient heating rate W_H will cause great errors in the experimental study. In most cases, heating time t_H was used instead of W_H. In view of the preheating temperature for CO_2 gas shielded welding was more than 100 °C, t_H was set to 5 seconds for heating to 1320 °C from room temperature.

(3) Dwell time t_m during peak temperature

Dwell time t_m during peak temperature has a great influence on crystallite dimension and stability of austenite. In view of actual welding condition and high temperature endurance of thermocouple, t_m was selected for 0.5 second in this simulation.

Table 3. Parameters used in thermal simulation.

Peak temperature T_p	1320 °C
Dwell time t_m during peak temperature	0.5 s
Heating rate W_H	Expressed by heating time t_H
Cooling rate *Wc*	Expressed by cooling time $t_{8/5}$

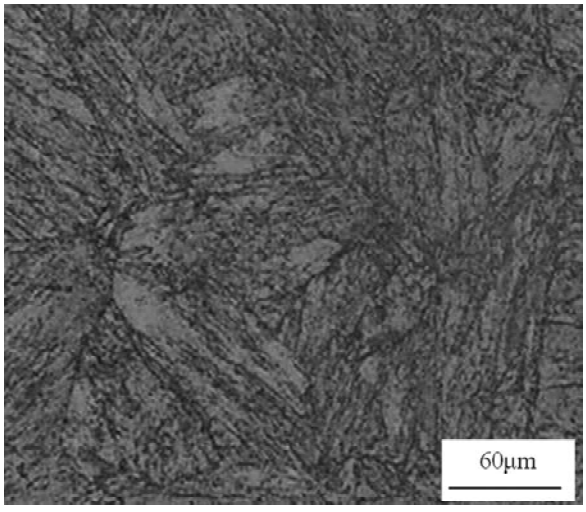

Fig. 1. Microstructure of high-strength wear-resistant steel NM360.

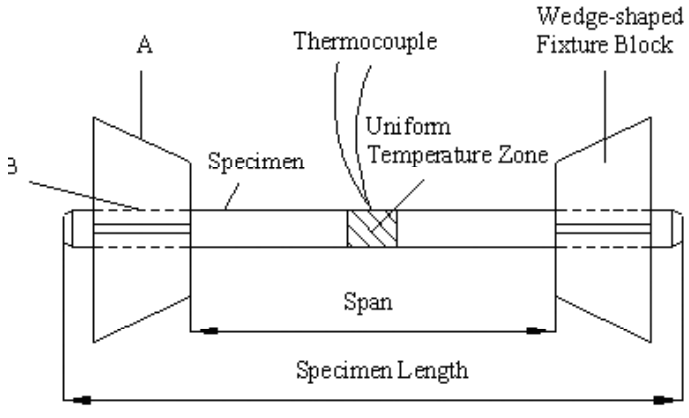

Fig. 2. Assembly diagram of test sample.

(4) Cooling rate *Wc*

For common low-alloy and high strength steel, microstructure in overheated zone depends on cooling velocity at 540 °C or cooling time $t_{8/5}$ (cooling time from 800 to 500 °C) because 800~ 500 °C are the most instable period for austenite and $t_{8/5}$ will finally decide the phase transition products in HAZ. Cooling time $t_{8/5}$ is used instead of cooling rate *Wc* because it is difficult to measure every transient temperature. It is set to 5, 10, 15, 20, 25, 30, 40, 50, 60 s by referring to the following factors: critical cooling time for appearance of intermediate structure, ferrite and pearlite; martensite transformation temperature M_s and M_f; maximum range of $t_{8/5}$ in CO_2 gas shielded welding.

Specimen is installed in the test groove of Gleeble-1500D and thermocouple is welded at the uniform temperature zone. Simulated data of thermal cycle, expansion-time and expansion-temperature can be obtained by the software of Quiksim.

3. RESULTS AND ANALYSIS

3.1. Effect of cooling time on impact ductility

Impact specimens were made into charpy-V notch according to GB2650-89 with dimension of 10 mm×10 mm×55 mm after thermal simulation. Impact tests were preceded on JB-300 charpy impact machine tester at 25 °C. The results are shown in Table 4 and the relevant curve of A_{kv} is shown in Fig. 3.

It can be seen from Fig. 3 that A_{kv} is lower and it changes very little when $t_{8/5}$ ranges from 0 to 20 s. This is because all of the microstructures are brittle martensite which can be seen from Fig. 4a. A_{kv}

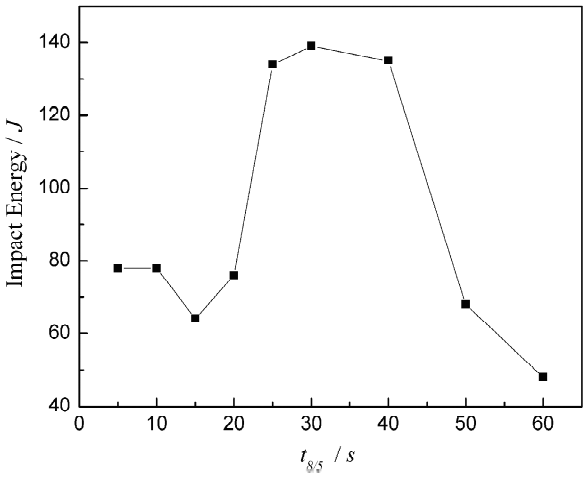

Fig. 3. Impact ductility of coarse-grain zone in HAZ for NM360.

reaches high value when $t_{8/5}$ ranges from 20 to 40 s. The reason for that is the appearance of martensite/bainite duplex structure which can be found in Fig. 4b and Fig. 4c. When $t_{8/5}$ is 30 s, A_{kv} reaches its maximum value 139 J. Researches [3-5] indicate that lower bainite/martensite duplex structure as well as non-carbide bainite/martensite duplex structure can improve both the ductility and strength. When it reaches a certain proportion for bainite and martensite, steel will be characterized by high strength and ductility. When $t_{8/5}$ exceeds 40 s, A_{kv} decreases obviously due to the plenty of bainite in coarse-grain zone, which can be seen in Fig. 4d. Though the A_{kv} decrease, all of the A_{kv} of the specimens are much higher than the base metal's (42 J).

3.2. Impact fracture in HAZ

Impact fractures of HAZ are analyzed through the scanning electron microscope S-570. It can be found in Figs. 5a and 5b that tearing ridges and river pat-

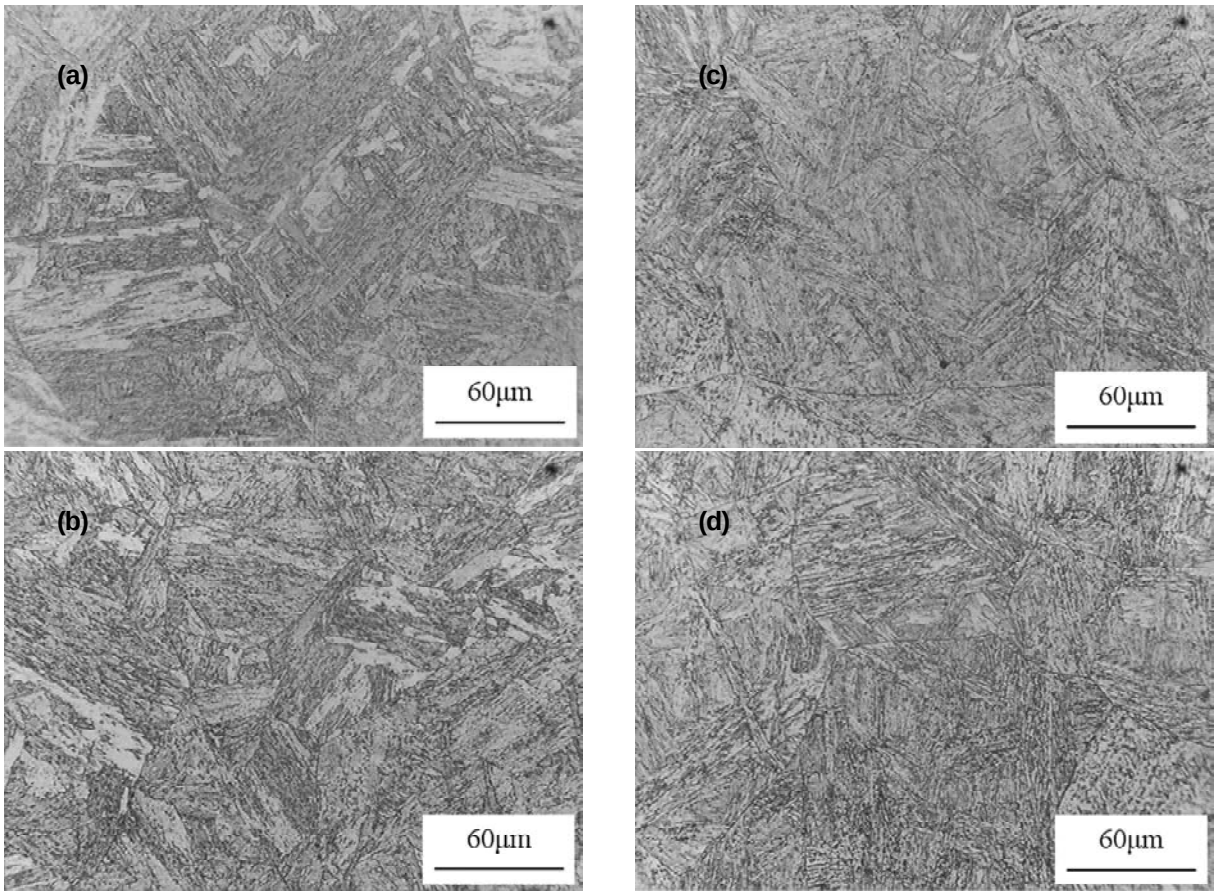

Fig. 4. Metallograph of coarse-grain zone in HAZ. a) $t_{8/5}$ = 5 s; b) $t_{8/5}$ = 19.7 s; c) $t_{8/5}$ = 30.6 s; d) $t_{8/5}$ = 50.7 s.

Table 4. Data of $t_{8/5}$ and A_{kv}.

Number	Default $t_{8/5}$ (s)	Actual $t_{8/5}$ (s)	A_{kv} (J)
D01	5	5.0	78
D02	10	10.9	78
D03	15	14.8	64
D04	20	19.7	76
D05	25	24.6	134
D06	30	30.6	139
D07	40	40.4	135
D08	50	50.7	68
D09	60	59.9	48

terns exist in all of the fractures when $t_{8/5}$ is less than 20 s. The reason is that the cooling rates are high and thus martensite transformation takes place. As is known to all, martensite is characterized by lower ductility and high hardness, so the quasi-cleavage fractures occur. When $t_{8/5}$ ranges from 20 to 40 s, all of the specimens are characterized by ductile fracture showing in Figs. 5c and 5d. This is because of the occurrence of bainite transformation then the duplex structure of martensite/bainite can improve steel's impact ductility. With the increasing of $t_{8/5}$, it turns into brittle fracture again, as is shown in Figs. 5e and 5f.

4. DISCUSSION

SH-CCT diagram has been widely used in welding which reflects the correlation between welding procedure and process of structure transformation in overheated zone. The process of phase transformation and its product can be forecasted by SH-CCT diagram under giving welding condition (*i.e.* $t_{8/5}$). Conversely, in order to achieve the optimal

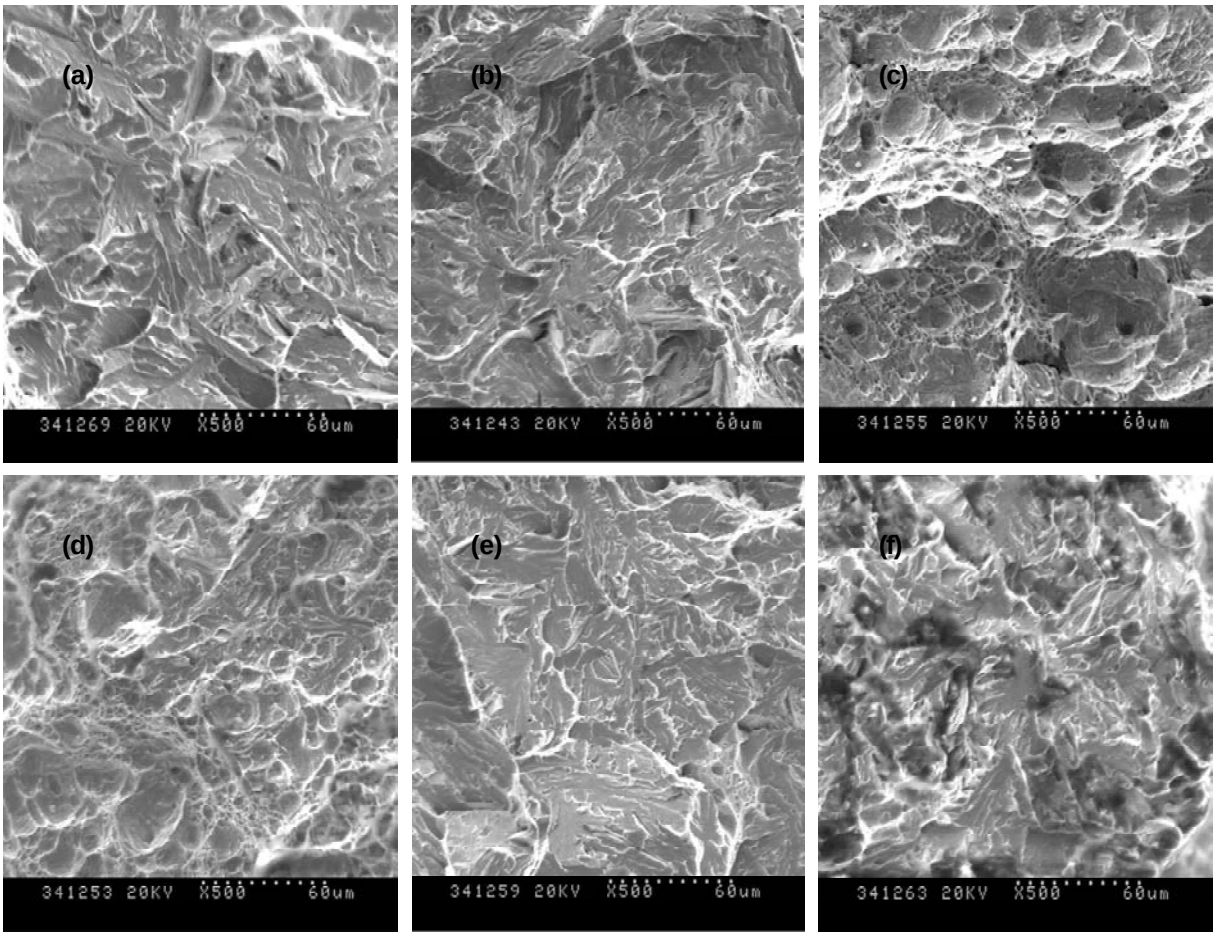

Fig. 5. SEM picture of impact fracture under different cooling rate in HAZ. a) $t_{8/5}$ = 5 s; b) $t_{8/5}$ = 14.8 s; c) $t_{8/5}$ = 24.6 s; d) $t_{8/5}$ = 40.4 s; e) $t_{8/5}$ = 50.7 s; f) $t_{8/5}$ = 59.9 s.

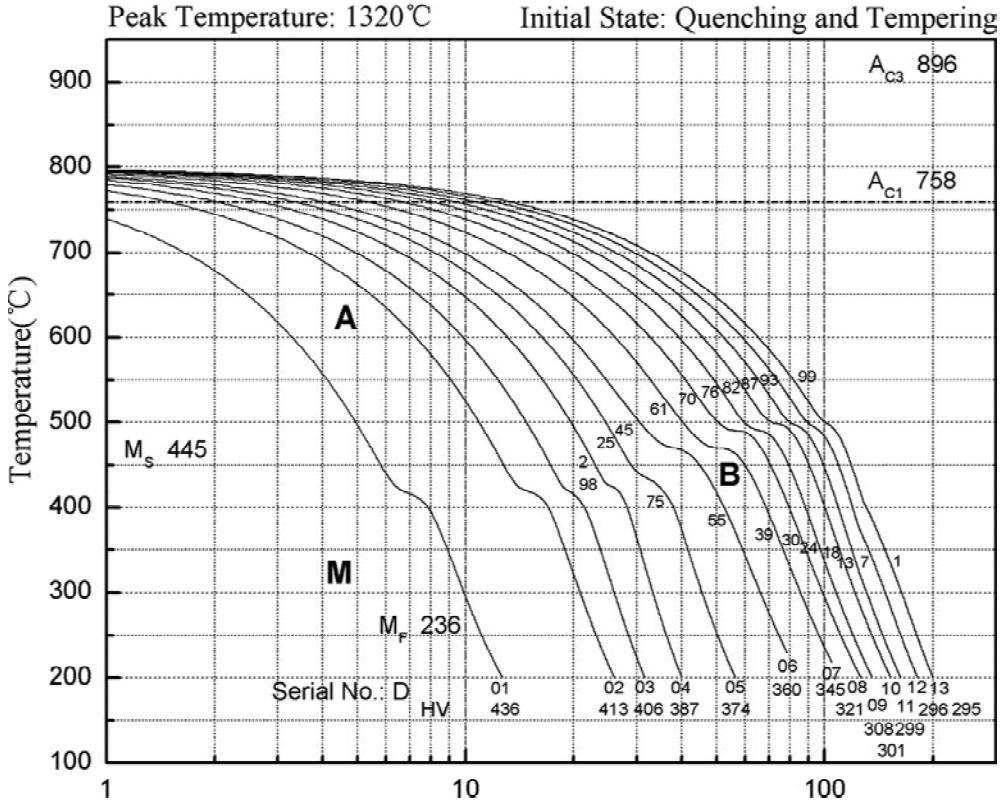

Fig. 6. Simulated HAZ continuous cooling transformation diagram (SH-CCT) of NM360 steel.

welding parameters, cooling curve, which relates to structure and performance, can be chose from SH-CCT diagram [6].

It can be seen from Fig. 3 and Fig. 6 that it is appropriate for $t_{8/5}$ ranging from 20 to 30 s for the welding of NM360 steel. In HAZ coarse-grain zone, structure is composed of a great quantity of low carbon martensite and a little bainite (2~45%) at this cooling rate. This area has an excellent combination property with high impact ductility (76~139 J) and hardness (HV387~HV360).

In the meanwhile, many other investigations [7] indicate that HAZ will become brittle in the weld of high strength, low carbon, low alloy, as well as hardened and tempered steel at low cooling rate. Because there are lots of upper bainite, martensite and bainite under low cooling rate. By improving heat input, the damage of HAZ can be avoided. Similarly, cold crack can be avoided by preheating noting that it may lead to lower cooling rate which may result in structure brittleness, strength decrease and bad toughness. Excellent toughness and cold crack resistant ability of HAZ can be obtained by lower heat-input, appropriate preheated temperature and improvement of the $t_{8/5}$. With reasonable welding parameters and high cooling rate, excellent mechanical property of HAZ can be achieved without post weld heat treatment.

5. CONCLUSION

(1) With the increasing of cooling rate, impact ductility of coarse-grain zone in HAZ will increase at first and then drop for NM360 steel. The best impact ductility can be achieved when $t_{8/5}$ varies between 25 and 40 s and the corresponding A_{kv} ranges from 134 to 139 J.

(2) With the increasing of cooling rate, the evolution of impact fracture is as follows: quasi-cleavage fracture ! dimple fracture ! quasi-cleavage fracture. That is coincident with the evolution of impact ductility in this area.

(3) The structure evolution and impact ductility in HAZ coarse-grain zone of NM360 steel can provide an important basis to the selection of welding technological parameters and forecast the joint's performance via welding procedure.

REFERENCES

[1] Z. Junjie, Z. Hanhua and X. Changmo // *J. Wuhan Univ. Technol.* **30** (2006) 395.

[2] N. Jitai, *Physical Simulation in Materials and Hot-working* (National Defence Industry Press, Beijing, 1999).

[3] Y. Fubao, B. Binzhe and L. Dongyu // *Acta Metall. Sinica.* **40** (2004) 296.

[4] Y. Tomitay // *Mater. Sci. Technol.* **7** (1991) 299.

[5] C. H. Young and H. K. D. H Bhadeshia // *Mater. Sci. Technol.* **10** (1994) 209.

[6] L. Deyuan, Z. Zhengfeng and S. Daqian // *J. Mater. Sci. Technol.* **14** (1998) 147.

[7] Y. Shike W. Yishan and G. Huaili // *Trans. China Weld. Inst.* **17** (1996) 25.